I&EC research
Industrial & Engineering Chemistry Research

Vapor-Phase Hydrogenolysis of Glycerol to 1,2-Propanediol over Cu/Al$_2$O$_3$ Catalyst at Ambient Hydrogen Pressure

M. L. Dieuzeide,[†] M. Jobbagy,[‡] and N. Amadeo[*,†]

[†]ITHES (UBA-CONICET, Laboratorio de Procesos Catalíticos, Departamento de Ing. Química, Facultad de Ingeniería, Universidad de Buenos Aires, Pabellón de Industrias, Ciudad Universitaria, 1428 Ciudad Autónoma de Buenos Aires, Argentina

[‡]INQUIMAE. Facultad de Ciencias Exactas y Naturales, Universidad de Buenos Aires, Pabellón II, Ciudad Universitaria, 1428 Ciudad Autónoma de Buenos Aires, Argentina

ABSTRACT: In this paper, we report that the hydrogenolysis of glycerol can be carried out at atmospheric pressure and low temperature with high selectivity to 1,2-PDO over reduced copper catalyst. The vapor-phase reaction was carried out over the copper-based catalysts supported on alumina at ambient pressure, and the effects of temperature, space time, and H$_2$ molar fraction in the feed were analyzed. The textural and structural characteristics of the catalysts with increasing copper loading were determined by N$_2$ sorptometry (BET), inductively coupled plasma-atomic spectroscopy (ICP-AES), powder X-ray diffraction (PXRD), temperature-programmed reduction (TPR), and N$_2$O chemisorption (metallic area). On the basis of both characterization and activity results, it was possible to conclude that the hydrogenolysis of glycerol to 1,2-propanediol in vapor phase at atmospheric pressure over copper-based catalysts is a structure sensitive reaction. Activity results suggests that the most probable pathway for the glycerol conversion into 1,2-propanediol under the employed conditions is glycerol is dehydration to hydroxyacetone (acetol), followed by its hydrogenation into 1,2-propanediol. Complete glycerol conversion and a selectivity of 60% to 1,2-propanediol was achieved, using CuO(15)Al$_2$O$_3$ catalyst at 200 °C, H$_2$ molar fraction of 61%, and atmospheric pressure.

1. INTRODUCTION

In recent years, biodiesel has gained attention as an attractive biofuel, especially because it can replace significant fractions of petroleum-derived fuels. This green vector is mainly produced by the transesterification of vegetable oils and fats, with glycerol being the major byproduct (10 wt % of production).

The growth in biodiesel production has caused an overproduction of glycerol. Consequently, glycerol became a low-cost building block with high potential, which could be employed to produce other chemicals with high added value.[1]

Among the different alternatives to add value to glycerol, the catalytic production of 1,2-propanediol (1,2-PDO) by hydrogenolysis of bioglycerol is of great interest because of the renewable character of this route. Traditionally, 1,2-PDO is produced by the hydration of propylene oxide or ethylene oxide derived from propylene or ethylene.[2]

One of the applications of 1,2-PDO is as a functional fluid, such as those for antifreeze, deicing, and heat transfer.[3] The market of antifreezing and deicing products derived from 1,2-PDO is growing as a consequence of the concern over the toxicity of ethylene glycol.[3]

In the presence of a metallic catalyst and hydrogen, depending mainly on reaction conditions and catalyst characteristics, glycerol can be converted to 1,2-PDO, 1,3-PDO, and ethylene glycol.[4,5]

The catalysts employed for hydrogenolysis of glycerol to 1,2-PDO are based on metals such as Ru, Pd, Rh, and Cu.[2,3,6−11] In contrast to noble metal catalysts that present low selectivity to 1,2-PDO because of the cleavage of C−C bond, copper-based catalysts combine high glycerol conversion with high selectivity to 1,2-PDO.[2,13] Copper is well-known for its low ability to break the C−C bonds of the glycerol molecule, resulting in minor formation of undesired products and major efficiency for C−O hydro-dehydrogenation reactions.[13,14]

Various supports including Cr$_2$O$_3$,[15] ZnO,[16,17] SiO$_2$,[17] and Al$_2$O$_3$[19] have been explored. Xiao et al.[15] found that glycerol hydrogenolysis occurs via a two-site mechanism over Cu−Cr catalyst in liquid phase. Previous reports[16,17] showed that hydrogenolysis to 1,2-PDO on Cu/ZnO-supported catalysts proceeds via dehydration of glycerol to acetol on the acid sites of the support. Recently Vasiliadou et al.[18] have demonstrated in their studies in liquid phase at high pressure over Cu/SiO$_2$ catalysts that SiO$_2$ does not exhibit catalytic activity in the glycerol hydrogenolysis. Vila et al.[19] have found that Al$_2$O$_3$ support is not involved in glycerol activation and that copper species are responsible for selectively converting the glycerol.

The main concern reported in literature with the reaction in liquid phase is the high pressure employed in order to increase hydrogen solubility to obtain higher selectivity to 1,2-PDO.[3] In the liquid-phase hydrogenolysis of glycerol, high reaction pressure is the common drawback. Gas-phase hydrogenolysis has also been studied recently[10,10,20,21] as the natural alternative scenario. Akiyama et al.[10,11] have reported that 1,2-PDO can be formed from glycerol with high selectivity over supported Cu/Al$_2$O$_3$ catalyst at ambient pressure by the application of a temperature gradient over the catalytic bed because of the hydrogenation of acetol to 1,2-PDO is thermodynamically

A

76 favored at lower temperatures. Feng et al.[21] have found that
77 Cu/ZnO/Al$_2$O$_3$ and Cu/ZnO/ZrO$_2$ exhibit good glycerol
78 conversion but low selectivity toward 1,2-PDO in the gas-
79 phase hydrogenolysis of glycerol under 0.1 MPa of H$_2$.

80 Considering that gas-phase hydrogenolysis of glycerol is a
81 potential alternative to that in liquid phase from the viewpoint
82 of the process cost; in this paper, we reported that 1,2-PDO can
83 be produced at atmospheric pressure and low temperature with
84 high selectivity from glycerol dehydrogenation. To achieve this
85 goal, the loading of copper supported on alumina was varied
86 between 3 and 20 wt % CuO, and the effects of temperature,
87 space time and H$_2$ molar fraction in the feed were analyzed.

2. EXPERIMENTAL SECTION

88 **2.1. Catalysis Preparation.** Catalysts with different CuO
89 contents supported over γ-Al$_2$O$_3$ were prepared by incipient
90 wetness impregnation method with aqueous solutions of
91 Cu(NO$_3$)$_2$·3H$_2$O (99.5% Merck, 1.5 and 10.1 M).

92 The employed catalyst support was γ-Al$_2$O$_3$ (Alumina
93 Harshaw Chemical Co., AL-0104 T 1/8 in.), being previously
94 crushed and sieved in order to obtain particles with diameters
95 between 44 μm < dp <125 μm. Before the impregnation with
96 copper salt, the bare γ-alumina was calcined in a muffle at 700
97 °C for 6 h in order to eliminate the OH$^-$ groups from the
98 surface and to stabilize the alumina phase.

99 After impregnation of alumina with Cu(NO$_3$)$_2$ solutions,
100 samples were dried at 120 °C for 6 h and then calcined at 400
101 °C for another 6 h; both stages were carried out in a muffle.
102 The temperature ramp employed during both drying and
103 calcination stages was 10 °C/min.

104 Catalysts were identified as CuO(x)/Al$_2$O$_3$, being x the
105 nominal content of CuO (wt %) between x = 3 and 20 wt %.

106 **2.2. Catalysts Characterization.** Fresh catalyst samples
107 were characterized by N$_2$ sorptometry (BET), inductively
108 coupled plasma-atomic spectroscopy (ICP-AES), temperature-
109 programmed reduction (TPR), and N$_2$O chemisorption
110 (metallic area).

111 Additionally, fresh and reduced catalysts samples were
112 characterized by powder X-ray diffraction (PXRD).

113 N$_2$ sorptometry (BET) was carried out in a Micromeritics
114 equipment ASAP 2020. For each analysis, a sample mass of 100
115 mg was employed.

116 The catalyst composition was determined in a Sequential
117 Plasma Spectrometer ICP-AES Shimadzu 1000 III. Solid
118 samples (known mass) were dissolved in a known volume of
119 nitric acid (65 wt %) by means of hydrothermal aging (24 h,
120 150 °C).

121 Characterization by powder X-ray diffraction (PXRD) was
122 carried out with Siemens D5000 equipment, employing Cu Kα
123 radiation.

124 Temperature-programmed reduction (TPR) of fresh samples
125 was carried out in a Micromeritics Autochem II 2920, with a
126 thermic conductivity detector (TCD). The samples (100 mg)
127 were placed in a quartz U-shaped reactor. Prior to temperature-
128 programmed reduction, samples were pretreated under a flow
129 of Ar (50 mL/min) at 200 °C for 1 h. TPR was carried out
130 from 50 to 400 °C at a heating rate of 10 °C/min, under a flow
131 of 100 mL/min of a mixture 2% H$_2$/Ar. Hydrogen
132 consumption was determined by a TCD detector, and the
133 amount of hydrogen consumed was estimated by the
134 integration of the TPR profiles and the application of H$_2$
135 calibration with 2 as stoichiometric factor.

136 The dissociative N$_2$O adsorption method was carried out in a
137 Micromeritics Autochem II 2920 in order to determine copper
138 metallic area, dispersion and particle size. The catalysts sample
139 (100 mg) was placed in a U-shaped quartz reactor and was
140 pretreated in flowing Ar (50 mL/min)at 100 °C for 30 min,
141 followed by cooling at room temperature. The catalyst
142 prereduction, was carried out increasing the temperature to
143 300 °C with a ramp of 10 °C/min under a 2% H$_2$/Ar (100 mL/
144 min) flow for 30 min. Then the sample was cooled to 50 ± 5
145 °C in Ar flow (50 mL/min) and sequentially was exposed to a
146 50% N$_2$O/Ar flow (100 mL/min) for 1 h, in order to oxidize
147 the Cu^0 to Cu$_2$O by dissociative adsorption of N$_2$O. Finally,
148 after the purged of the sample under Ar flow (50 mL/min) at
149 50 °C for 15 min, the TPR was carried out in order to reduce
150 the Cu$_2$O species to metallic copper. This stage was carried out
151 in a 2% H$_2$/Ar flow (100 mL/min), and temperature was
152 increased to 300 °C with a 10 °C/min ramp. The copper
153 metallic area, dispersion, and particle size were calculated on
154 the basis of refs 22 and 23, considering that the number of
155 superficial copper atoms per unit surface area is 1.47 × 10^{19}
156 atoms/m^2, and the density of copper is 8.92 g/cm^3.

157 **2.3. Catalytic Activity.** Glycerol hydrogenolysis was carried
158 out in a stainless-steel continuous-flow fixed-bed reactor (Ø =
159 12 mm) at atmospheric pressure in an electrical furnace
160 equipped with temperature controllers. Reaction temperature
161 was measured with a k-type thermocouple placed in the middle
162 of the catalytic bed. For all catalytic tests, the liquid stream was
163 fed with a HPLC pump (Eldex 1HM) and was vaporized in the
164 first third of the reactor; the liquid feed stream consisted of a
165 water glycerol mixture with molar ratio ($R = n_{H_2O}/n_{C_3H_8O_3}$) R =
166 9:1 (35 wt % glycerol aqueous solution). Reactions were carried
167 out isothermally at 200 or 240 °C, and contact time varied
168 between 30 and 180 g$_{cat}$ h/mol. Normally, the hydrogen to
169 glycerol molar ratio employed was 65:1; however, when the
170 effect of hydrogen partial pressure was analyzed, this ratio was
171 varied between 43:1 and 87:1. The feed stream was completed
172 with Ar. Both the carrier gas (Ar) and hydrogen were fed to the
173 reaction system by mass flow controllers (Brooks 0254).

174 Catalysts were reduced in situ at 300 °C under a flow of 50%
175 H$_2$/Ar (100 mL/min) during the first 30 min and under a flow
176 of pure hydrogen (100 mL/min) for another 30 min. The
177 heating ramp employed to reach 300 °C was 10 °C/min. Then,
178 the catalytic bed temperature was set at reaction temperature
179 (200 or 240 °C) under a flow of Ar. The total flow rate and
180 particle diameter were chosen in order to guarantee the absence
181 of diffusional resistance during reaction tests.

182 Both liquid feed samples and condensed samples were
183 analyzed by a GC (Agilent Technologies 7890A, DB-5, 30 m ×
184 0.320 mm × 0.5 μm). Liquid samples were collected every hour
185 during reaction. The internal standard method was used for the
186 quantification of the results, with n-butanol being the standard.
187 The liquid products analyzed were 1,2-propanediol (propylene
188 glycol), 1,3-propanediol, ethylene glycol, and hydroxyacetone
189 (acetol); no propanol was detected in the condensed stream.
190 Gas stream was analyzed by a GC (Agilent Tecnologies 6890N,
191 Carboxen 1010 Plot, 30 m × 0.53 mm); however, no gaseous
192 products were detected except for nonreacted hydrogen.

193 To analyze the catalytic results, the following parameters
194 were considered:

Glycerol conversion: x_G

$$= \frac{[\text{moles of glycerol}]_{in} - [\text{moles of glycerol}]_{out}}{[\text{moles of glycerol}]_{in}} 100$$

Yield: $Y_i = \frac{[\text{moles of one product}]_{out}}{[\text{moles of glycerol}]_{in}} 100$

Selectivity:

$$S_i = \frac{[\text{moles of one product}]_{out}}{[\text{moles of glycerol}]_{in} - [\text{moles of glycerol}]_{out}} 100$$

Activity tests took place for 6 h under reaction conditions. In addition, carbon balance in all experiments was 100 ± 5%.

3. RESULTS AND DISCUSSION

3.1. Characterization. The composition together with the surface area of the catalysts and support are summarized in Table 1. The decrease in surface area observed for the catalyst

Table 1. CuO(x)/Al$_2$O$_3$ Catalysts BET Surface Area and ICP Results with x = 0−20 wt %

| | nominal CuO (wt %) | BET area (m^2/g) | ICP analysis | | |
			Cu/Al	real CuO (wt %)	relative error (%)
γ-Al$_2$O$_3$		93.4			
CuO(03)/Al$_2$O$_3$	3.0	90.2	0.05	3.4	12.6
CuO(05)/Al$_2$O$_3$	5.0	90.5	0.08	4.9	1.2
CuO(07)/Al$_2$O$_3$	7.0	91.2	0.11	7.2	2.9
CuO(10)/Al$_2$O$_3$	10.0	88.2	0.16	10.3	3.3
CuO(15)/Al$_2$O$_3$	15.0	77.2	0.24	15.9	5.8
CuO(20)/Al$_2$O$_3$	20.0	78.0	0.31	20.6	2.8

samples supported on Al$_2$O$_3$ compared with that for bare support reveals the textural effect of copper impregnation. The agreement between the theoretical copper content and the estimated by ICP analysis is satisfactory, except for that with CuO(03)/Al$_2$O$_3$ catalyst. This suggests that in most of the samples prepared all the copper used for the impregnation was incorporated to the alumina.

In Figure 1, the powder X-ray diffraction patterns of fresh samples are shown. All the XRD patterns show broad diffraction peaks corresponding to ill-crystallized γ-alumina. The more intense reflections corresponding to CuO (2θ values 35.5 and 38.8) are visible for catalysts with copper loading equal or higher than 5 wt %. No diffraction peaks corresponding to copper-containing phases were observed for CuO(03)/Al$_2$O$_3$ catalyst. The absence of CuO diffraction peaks would indicate the formation of highly dispersed copper species that are not detectable by this technique on the alumina surface.

The powder X-ray diffraction patterns of catalyst-reduced samples are presented in Figure 2. In agreement with the PXRD diffraction patterns of the fresh samples, the reflections corresponding to Cu^0 (2θ values 43.3, 50.4, and 74.1°) are visible for catalyst with copper loadings higher than 5 wt %. Additionally, the intensity of the diffraction reflection associated with Cu^0 increased with copper loading. All the samples presented the characteristic diffraction peak associated with γ-alumina.

The redox properties of the catalyst were studied by TPR technique. The reduction profiles of all catalysts (Figure 3) are
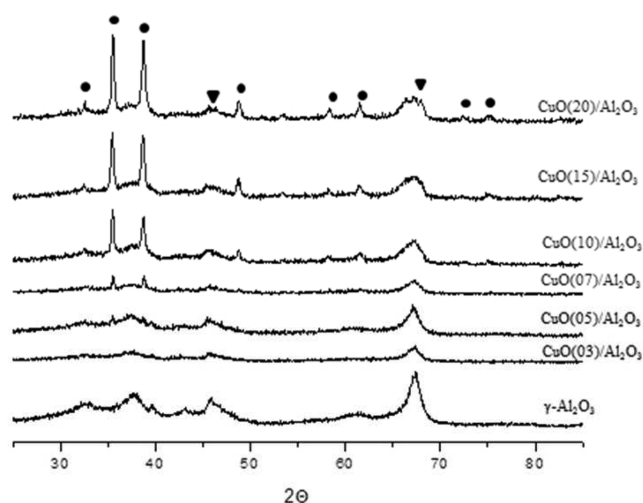
Figure 1. XRD profiles of CuO(x)/Al$_2$O$_3$ fresh catalysts, with x = 0− 20 wt % (●) CuO and (▼) Al$_2$O$_3$.
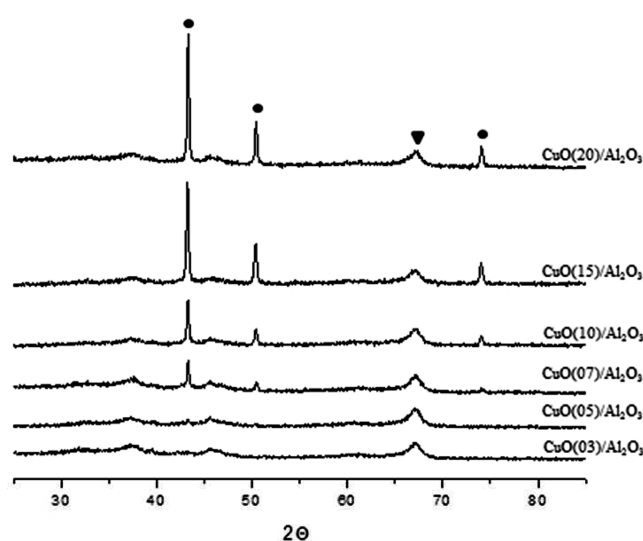
Figure 2. XRD profiles of CuO(x)/Al$_2$O$_3$ reduced catalysts, with x = 0−20 wt %. (●) Cu^0 and (▼) Al$_2$O$_3$.
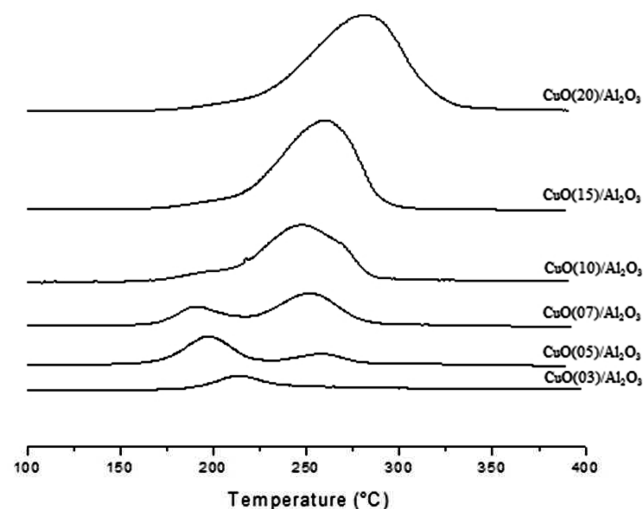
Figure 3. TPR profiles of CuO(x)/Al$_2$O$_3$ catalysts, with x = 3−20 wt %.

related with copper oxide reduction. As expected, the higher the copper loading, the higher the H_2 consumed. Most of TPR profiles show two reduction signals, indicating that there are two copper oxide species with different redox behavior. Typically, the β peak (around 210 °C) obeys the reduction of highly dispersed copper oxide species, whereas the α peak (around 260 °C) relates to the reduction of bulklike CuO phases.[24,25] The α peak area increases with copper loading, whereas the β peak area has a maximum for CuO(05)/Al$_2$O$_3$ catalyst. For copper loadings equal or lower than 5 wt %, the proportion of β copper is higher, whereas this proportion decreases as copper loading increases accompanied by the increment in α proportion.

N$_2$O chemisorption experiments enabled us to determine the copper metallic surface area, dispersion, and particle diameter for all catalysts. As expected, the results in Table 2 show that copper particle diameter increases as copper loading increases (Figure 4).

Table 2. N$_2$O Chemisorption Results for CuO(x)/Al$_2$O$_3$ Reduced Catalysts with x = 3−20 wt %

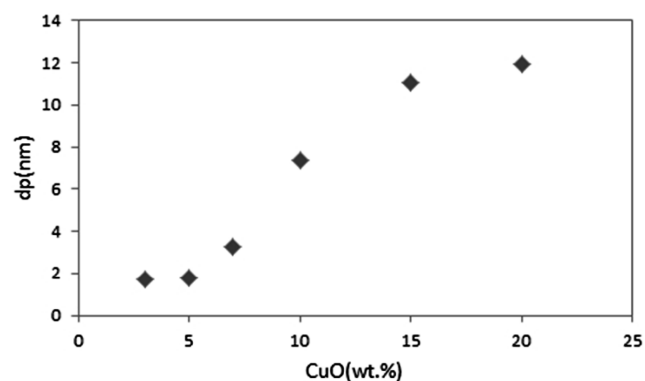|	S$_{Cu}$ (m^2/g Cu)	D (%)	dp (nm)
CuO(03)/Al$_2$O$_3$	392	60.9%	1.7
CuO(05)/Al$_2$O$_3$	377	58.5%	1.8
CuO(07)/Al$_2$O$_3$	206	32.0%	3.3
CuO(10)/Al$_2$O$_3$	91	14.1%	7.4
CuO(15)/Al$_2$O$_3$	61	9.4%	11.0
CuO(20)/Al$_2$O$_3$	56	8.7%	11.9

Figure 4. Copper metallic particle diameter vs copper loading for catalysts CuO(x)/Al$_2$O$_3$ with x = 3−20 wt %.

3.2. Reaction. 3.2.1. Effect of Cu Loading. Figure 5 shows glycerol conversion measured for the catalysts with different copper content at 240 °C. Glycerol conversion has a maximum with the CuO loading, reaching this maximum for a copper loading between 7 and 15 wt %. The products yields, in Figure 5, present the same trend with copper content as that with glycerol conversion. It is possible to emphasize that the only products detected were acetol, 1,2-PDO, ethylene glycol, and traces of 1,3-PDO.

In addition to these results, it is important to mention that a catalytic test was carried out with bare γ-Al$_2$O$_3$ (previously calcined at 700 °C) under the same reaction conditions as those of the results shown in Figure 5. Glycerol conversion under these reaction conditions over bare γ-Al$_2$O$_3$ was lower than 5%, and the main product was acetol.
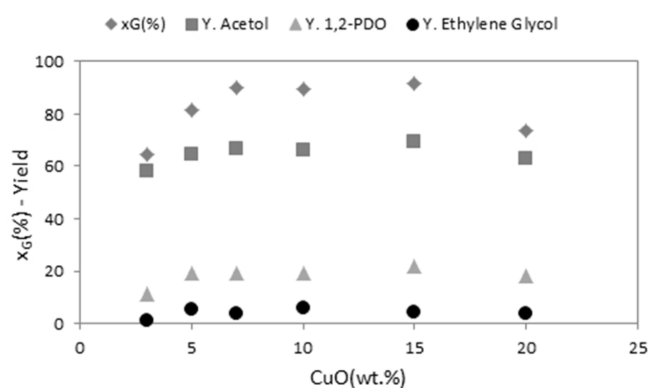

Figure 5. Glycerol conversion and yields to acetol, 1,2-PDO, and ethylene glycol vs CuO (wt %) content at 240 °C, P = 1 atm, yH$_2$ = 61%, and contact time 30 gcat min/mol. Catalysts CuO(x)/Al$_2$O$_3$, with x = 3−20 wt %.

In agreement with our results, it is known that copper is an active metal for both dehydration and hydrogenation reactions.[14,15] In particular, glycerol conversion occurs when copper is present, suggesting that these copper species participate in glycerol activation. The intrinsic activity, defined as glycerol conversion per active Cu site, was compared with metallic copper particle size (Figure 6). The strong dependence
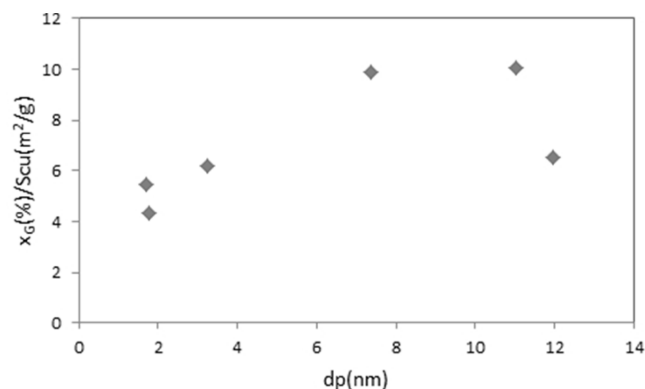

Figure 6. Glycerol conversion ratio to copper metallic area vs copper particle size (nm) content at 240 °C, P = 1 atm, yH$_2$ = 61%, and contact time 30 gcat min/mol. Catalysts CuO(x)/Al$_2$O$_3$, with x = 3−20 wt %.

observed suggests that the present is a structure sensitive reaction as was reported by other authors.[18,20,26,27] Finally it is important to note that all catalysts were stable during the 6 h of the catalytic activity test. Stability results shown in Figure 7 are representative of all the activity tests carried out.

3.2.2. Effect of Contact Time. CuO(15)/Al$_2$O$_3$ was chosen to optimize the yield of 1,2-PDO against contact time, H$_2$ molar fraction and reaction temperature.

First, experiments at different contact times, using different masses of CuO(15)/Al$_2$O$_3$ catalyst, were conducted. Product distribution is shown in Figure 8. These results suggest that acetol is an intermediate product because its yield presents a maximum with contact time, whereas 1,2-PDO is a final product because of the continuous increment in its yield. Even though it is difficult to elucidate the ethylene glycol behavior in the reaction pathway because of its very low production in the whole range of contact times considered, ethylene glycol could be formed by a parallel reaction from glycerol.[28]
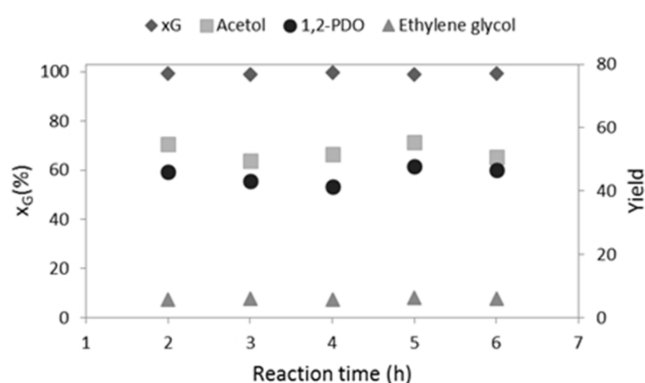
D

Figure 7. Glycerol conversion and yield to acetol, 1,2-PDO, and ethylenglycol vs reaction time at 240 °C, $P = 1$ atm, $yH_2 = 61\%$, and contact time 120 gcat min/mol over $CuO(15)/Al_2O_3$ catalyst.
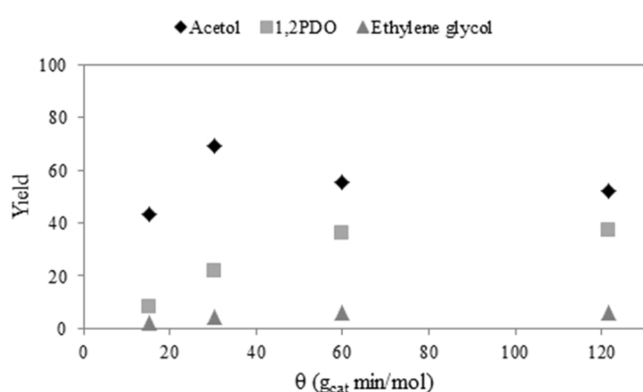

Figure 8. Yield to acetol, 1,2-PDO, and ethylene glycol vs contact time over $CuO(15)/Al_2O_3$ catalyst at 240 °C, $yH_2 = 61\%$, and $P = 1$ atm.

Consistent with these results, the selectivity to 1,2-PDO grows as contact time increases (Figure 9). Therefore, it could
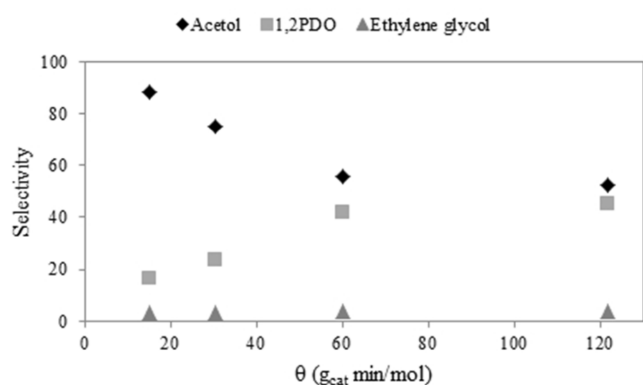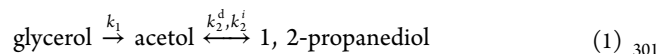

Figure 9. Selectivity to acetol, 1,2-PDO, and ethylene glycol vs contact time over $CuO(15)/Al_2O_3$ catalyst at 240 °C, $yH_2 = 61\%$, and $P = 1$ atm.

be concluded that high contact times favor the formation of 1,2-PDO, disfavoring the acetol production, and also confirms that 1,2-PDO is a secondary product of glycerol hydrogenolysis. Additionally, it could be inferred from these results that acetol besides being an intermediate product in the reaction pathway is a primary product because its selectivity tends to 100% when the contact time tends to 0.

The results presented in this section confirm in agreement with previous reports[3,28,29] that in this system the hydrogenolysis of glycerol occurs through the following system of series reactions: First, glycerol is dehydrated to give acetol, which is then hydrogenated to yield the 1,2-PDO. The reaction scheme is described by

$$\text{glycerol} \xrightarrow{k_1} \text{acetol} \underset{k_2^i}{\overset{k_2^d}{\rightleftharpoons}} 1,2\text{-propanediol} \qquad (1)$$

3.2.3. Effect of H_2 Molar Fraction. Figure 10 shows the effect of hydrogen molar fraction on glycerol dehydrogenation
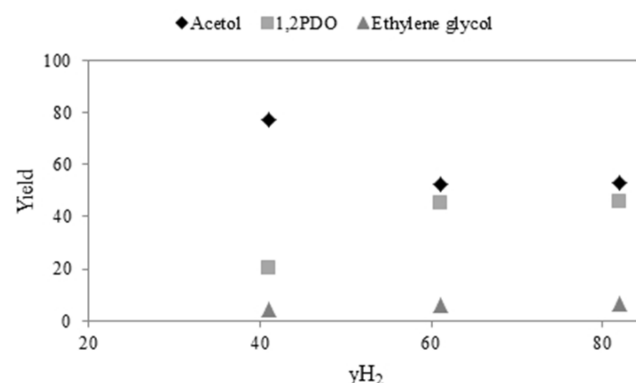

Figure 10. Yield to acetol, 1,2-PDO, and ethylene glycol vs hydrogen molar fraction in the feed at 240 °C, $P = 1$ atm, and contact time 120 gcat min/mol, over $CuO(15)/Al_2O_3$ catalyst.

at 240 °C and at 120 g_{cat} min/mol. The yield to 1,2-PDO increases with increasing H_2 molar fraction, and this value remains constant for a H_2 molar fraction equal or higher than 0.6. It is probable that chemical equilibrium is being achieved for this hydrogen molar fraction range and under the operating conditions considered.

3.2.4. Effect of Reaction Temperature. Finally, o study the optimum reaction conditions, the effect of reaction temperature on the hydrogenolysis of glycerol at ambient pressure and at contact time of 120 g_{cat} min/mol was considered. Table 3

Table 3. Glycerol Conversion and Selectivity to Acetol, 1,2-PDO and Ethylenglycol vs Temperature (200 and 240 °C)[a]

temperature (°C)	glycerol conversion	acetol selectivity	1,2-PDO selectivity	ethylenglycol selectivity
200	99.6	41.3	58.2	2.7
240	99.3	52.3	45.5	4.0

[a]$CuO(15)/Al_2O_3$ catalysts, $P = 1$ atm, $yH_2 = 61\%$, and contact time 120 gcat min/mol.

shows glycerol conversion and selectivity to reaction products at two different reaction temperatures. For both temperatures, the glycerol conversion is complete because of the high contact time employed. The selectivity to 1,2-PDO increases from 45.5 to 58.2% when temperature decreases from 240 to 200 °C at expense of the acetol selectivity. Low reaction temperature favors the hydrogenation of acetol to 1,2-PDO.

It is necessary to know whether the yield of 1,2-PDO at 200 °C is also limited by the equilibrium or if its production can be improved by increasing contact time. The results presented in Figure 11 reveal that the equilibrium has not been reached at 200 °C; therefore, the production of 1,2-PDO increases with
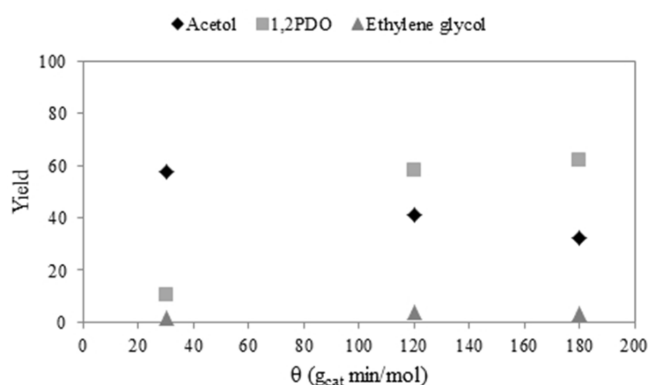
Figure 11. Yield to acetol, 1,2-PDO, and ethylenglycol vs contact time at 200 °C, $yH_2 = 61\%$, and $P = 1$ atm, over $CuO(15)/Al_2O_3$ catalyst.

contact time. It can be seen that under this operating condition the yield of 1,2-PDO doubles the one of acetol.

Complete conversion of glycerol and selectivity to 1,2-PDO of 58% was achieved over $CuO(15)/Al_2O_3$ catalyst at 200 °C, with contact time 180 g_{cat} min/mol and at atmospheric pressure. These are promising results because equilibrium for the hydrogenation of acetol was not reached, and selectivity to 1,2-PDO could be improved by increasing contact time or by reducing the reaction temperature.

4. CONCLUSIONS

The hydrogenolysis of glycerol in vapor phase at atmospheric pressure was studied on copper-based catalysts supported over alumina with increasing loadings of CuO. Glycerol conversion presents a maximum with the loading of copper, reaching the maximum conversion for a copper content between 7 and 15 wt %.

N_2O chemisorption experiments show that both the copper loading and copper metallic particle size follow the same trend: The higher the copper loading, the higher the copper particle size. The glycerol conversion per active Cu site depends strongly on copper metallic particle size, thus demonstrating the structure sensitivity of the glycerol dehydrogenation reaction.

The analysis of product distribution shows that acetol has a behavior of an intermediate and primary product, whereas 1,2-PDO is a final product.

1,2-PDO yield increased with increasing H_2 molar fraction up until a value of 0.6 of H_2 molar fraction. With further increases of the H_2 molar fraction, 1,2-PDO yield remained constant.

There is a trade-off problem between the glycerol dehydration and the acetol hydrogenation. High temperature favors glycerol dehydration, but the 1,2-PDO production increases as temperature decreases.

Finally, it was found that glycerol hydrogenolysis on copper-supported alumina catalyst with a copper loading of 15 wt % at 200 °C and atmospheric pressure with a contact time of 180 g_{cat} min/mol achieved complete conversion with 60% of selectivity to 1,2-PDO.

■ AUTHOR INFORMATION

Corresponding Author

*E-mail: norma@di.fcen.uba.ar.

Notes

The authors declare no competing financial interest.

■ REFERENCES

(1) Pagliaro, M.; Ciriminna, R.; Kimura, H.; Rossi, M.; Della Pina, C. From Glycerol to value-added products. *Angew. Chem., Int. Ed.* **2007**, *46*, 4434−4440.

(2) Chaminand, J.; Djakovitch, L.; Gallezot, P.; Marion, P.; Pinel, C.; Rosier, C. Glycerol hydrogenolysis on heterogeneous catalysts. *Green Chem.* **2004**, *6*, 359−361.

(3) Dasari, M. A.; Kiatsimkul, P.; Sutterlin, W. R.; Suppes, G. J. Low-pressure hydrogenolysis of glycerol to propylene glycol. *Appl. Catal., A* **2005**, *281*, 225−231.

(4) Kusunoki, Y.; Miyazawa, T.; Kunimori, K.; Tomishige, K. Highly active metal−acid bifunctional catalyst system for hydrogenolysis of glycerol under mild reaction conditions. *Catal. Commun.* **2005**, *6*, 645−649.

(5) Sato, S.; Akiyama, M.; Takahashi, R.; Hara, T.; Inui, K.; Yokota, M. Vapor-phase reaction of polyols over copper catalysts. *Appl. Catal., A* **2008**, *347*, 186−191.

(6) Huang, L.; Zhu, Y. L.; Zheng, H. Y.; Li, Y. W.; Zeng, Z. Y. Continuous production of 1,2-propanediol by the selective hydrogenolysis of solvent-free glycerol under mild conditions. *J. Chem. Technol. Biotechnol.* **2008**, *83*, 1670−1675.

(7) Yuan, Z.; Wang, J.; Wang, L.; Xie, W.; Chen, P.; Hou, Z.; Zheng, X. Biodiesel derived glycerol hydrogenolysis to 1,2-propanediol on Cu/MgO catalysts. *Bioresour. Technol.* **2010**, *101*, 7088−7092.

(8) Montassier, C.; Giraud, D.; Barbier, J. *Stud. Surf. Sci. Catal.* **1988**, *41*, 165−170.

(9) Montassier, C.; Dumas, J. M.; Granger, P.; Barbier, J. Deactivation of supported copper based catalysts during polyol conversion in aqueous phase. *Appl. Catal., A* **1995**, *121*, 231−244.

(10) Sato, S.; Akiyama, M.; Inui, K.; Yokota, M. Selective Conversion of Glycerol into 1,2-Propanediol at Ambient Hydrogen Pressure. *Chem. Lett.* **2009**, *38*, 560−561.

(11) Akiyama, M.; Sato, S.; Takahashi, R.; Inui, K.; Yokota, M. Dehydration−hydrogenation of glycerol into 1,2-propanediol at ambient hydrogen pressure. *Appl. Catal., A* **2009**, *371*, 60−66.

(12) Guo, L.; Zhou, J.; Mao, J.; Guo, X.; Zhang, S. Supported Cu catalysts for the selective hydrogenolysis of glycerol to propanediols. *Appl. Catal., A* **2009**, *367*, 93−98.

(13) Maris, E. P.; Davis, R. J. Hydrogenolysis of glycerol over carbon-supported Ru and Pt catalysts. *J. Catal.* **2007**, *249*, 328−337.

(14) Wang, S.; Zhang, Y.; Liu, H. Selective Hydrogenolysis of Glycerol to Propylene Glycol on Cu−ZnO Composite Catalysts: Structural Requirements and Reaction Mechanism. *Chem. - Asian J.* **2010**, *5*, 1100−1111.

(15) Xiao, Z.; Wang, X.; Xiu, J.; Wang, Y.; Williams, C.; Liang, C. Synergetic effect between Cu0 and Cu+ in the Cu-Cr catalysts for hydrogenolysis of glycerol. *Catal. Today* **2014**, *234*, 200−207.

(16) Balaraju, M.; Rekha, V.; Sai Prasad, S.; Prasad, R. B. N.; Lingaiah, N. Selective Hydrogenolysis of Glycerol to 1, 2 Propanediol Over Cu−ZnO Catalysts. *Catal. Lett.* **2008**, *126*, 119−124.

(17) Wang, S.; Liu, H. Selective hydrogenolysis of glycerol to propylene glycol on Cu−ZnO catalysts. *Catal. Lett.* **2007**, *117*, 62−67.

(18) Vasiliadou, E.; Eggenhuisen, T.; Munnik, P.; de Jongh, P.; de Jong, K. P.; Lemonidou, A. Synthesis and performance of highly dispersed Cu/SiO2 catalysts for the hydrogenolysis of glycerol. *Appl. Catal., B* **2014**, *145*, 108−119.

(19) Vila, F.; Lopez Granados, M.; Ojeda, M.; Fierro, J. L. G.; Mariscal, R. Glycerol hydrogenolysis to 1,2-propanediol with Cu/γ-Al_2O_3: Effect of the activation process. *Catal. Today* **2012**, *187*, 122−128.

(20) Bienholz, A.; Hofmann, H.; Claus, P. Selective hydrogenolysis of glycerol over copper catalysts both in liquid and vapour phase: Correlation between the copper surface area and the catalyst's activity. *Appl. Catal., A* **2011**, *391*, 153−157.

434 (21) Feng, Y.; Yin, H.; Wang, A.; Shen, L.; Yu, L.; Jiang, T. Gas phase
435 hydrogenolysis of glycerol catalyzed by $Cu/ZnO/MO_x$ (MO_x =
436 Al_2O_3, TiO_2, and ZrO_2) catalysts. *Chem. Eng. J.* **2011**, *168*, 403−412.
437 (22) Sato, S.; Takahashi, R.; Sodesawa, T.; Yuma, K.; Obata, Y.
438 Distinction between Surface and Bulk Oxidation of Cu through N_2O
439 Decomposition. *J. Catal.* **2000**, *196*, 195−199.
440 (23) Gervasini, A.; Bennici, S. Dispersion and surface states of copper
441 catalysts by temperature-programmed-reduction of oxidized surfaces
442 (s-TPR). *Appl. Catal., A* **2005**, *281*, 199−205.
443 (24) Dow, W.; Wang, Y.; Huang, T. TPR and XRD studies of yttria-
444 doped ceria/g-alumina-supported copper oxide catalyst. *J. Catal.* **1996**,
445 *160*, 155−170.
446 (25) Lopez-Suarez, F. E.; Bueno-Lopez, A.; Illán-Gómez, M. J. Cu/
447 Al_2O_3 catalysts for soot oxidation: Copper loading effect. *Appl. Catal.,*
448 *B* **2008**, *84*, 651−658.
449 (26) Huang, Z.; Liu, H.; Cui, F.; Zuo, J.; Chen, J.; Xia, Ch. Effects of
450 the precipitation agents and rare earth additives on thestructure and
451 catalytic performance in glycerol hydrogenolysis of Cu/SiO_2 catalysts
452 prepared by precipitation-gel method. *Catal. Today* **2014**, *234*, 223−
453 232.
454 (27) Vasiliadou, E. S.; Lemonidou, A. A. Investigating the
455 performance and deactivation behaviour of silica-supported copper
456 catalysts in glycerol hydrogenolysis. *Appl. Catal., A* **2011**, *396*, 177−
457 185.
458 (28) Chiu, C. W.; Tekeei, A.; Ronco, J. M.; Banks, M. L.; Suppes, G.
459 J. Reducing Byproduct formation during Conversion of Glycerol to
460 Propylene Glycol. *Ind. Eng. Chem. Res.* **2008**, *47*, 6878−6884.
461 (29) Miyazawa, T.; Koso, S.; Kunimori, K.; Tomishige, K. Glycerol
462 hydrogenolysis to 1,2-propanediol catalyzed by a heat-resistant ion-
463 exchange resin combined with Ru/C. *Appl. Catal., A* **2007**, *329*, 30−
464 35.